J. Am. Chem. Soc. **1987**, *109*, 5780–5789

24-1; allyl alcohol, 107-18-6; (*s*)-2-methyloxiranemethanol 4-methylbenzenesulfinate (isomer 1), 106948-12-3; (*s*)-2-methyloxiranemethanol 4-methylbenzenesulfinate (isomer 2), 106948-13-4; cyclohexyl bromide, 108-85-0; cyclododecanol, 1724-39-6; L-(+)-diethyl tartrate, 87-91-2; (*E*)-2-hexen-1-ol, 928-95-0; (*Z*)-2-decen-1-ol, 4194-71-2; (*Z*)-2-undecen-1-ol, 75039-83-7; cumene hydroperoxide, 80-15-9; (*E*)-2-buten-1-ol, 504-61-0; *p*-nitrobenzoyl chloride, 122-04-3; *tert*-butyldiphenylsilyl chloride, 58479-61-1; 2-methyl-2-propen-1-ol, 513-42-8; 2-naphthalenesulfonyl chloride, 93-11-8; 3-methyl-2-buten-1-ol, 556-82-1; geraniol, 106-24-1.

Mechanism of the Gas-Phase Thermolysis of Monomethylsilane

P. S. Neudorfl,† E. M. Lown, I. Safarik, A. Jodhan, and O. P. Strausz*

Contribution from the Department of Chemistry, University of Alberta, Edmonton, Alberta, T6G 2G2, Canada. *Received December 9, 1986*

Abstract: The thermolysis of monomethylsilane (MMS) has been studied as a function of pressure (33–400 Torr), temperature (340–440 °C), and conversion. Under conditions of very low (typically, 0.5%) conversion and in a carefully seasoned vessel the major products are H_2 and dimethyldisilane (DMDS). Dimethylsilane (DMS) comprises ~5% of the major products. MMS-d_3 generates D_2 exclusively. In the presence of ~10% C_2H_4 the yields of H_2 and DMDS are considerably reduced and both products follow first-order kinetics in their formation. Also, the formation of DMS is completely suppressed, and the Arrhenius parameters for the molecular process $CH_3SiH_3 \rightarrow CH_3\ddot{S}iH + H_2$ (1a) when determined from the rate of H_2 production and from ($CH_3\ddot{S}iH + CH_3SiH_3 \rightarrow$ DMDS) production are $\log k_{1a} = (15.02 \pm 0.10) - (63270 \pm 310)/2.3RT$ and $(14.87 \pm 0.12) - (63150 \pm 350)/2.3RT$, respectively. The "molecular" rate constant for H_2, however, includes a small contribution from radical processes that cannot be completely suppressed. When the latter expression for k_{1a} is used, the rate data for H_2 in the unscavenged reaction can be fitted to a mechanism incorporating a second primary step, a slow, surface-catalyzed reaction generating $H^\bullet$ and $CH_3SiH_2^\bullet$ radicals, which then set up a short chain:

$$CH_3SiH_2^\bullet + CH_3SiH_3 \rightarrow \text{DMDS} + H$$

$$H + CH_3SiH_3 \rightarrow H_2 + CH_3SiH_2^\bullet$$

On the basis of kinetic analysis of the data it is concluded that the chain is terminated linearly by $CH_3SiH_2^\bullet$ radicals at the surface, with $\log A\ (s^{-1}) = 11.7$ and $E_a \approx 32.3$ kcal mol^{-1}. The derived rate expression for the surface-catalyzed radical initiation step $CH_3SiH_3 \rightarrow CH_3SiH_2^\bullet + H$ (1b) is $\log k_{1b} = 12.7 - 57900/2.3RT$. From the measured kinetic data the following thermochemical values were derived: $D(CH_3\ddot{S}iH\text{-}H) = 73.5$ kcal mol^{-1} and $\Delta H_f(CH_3\ddot{S}iH) = 51.9$ kcal mol^{-1}.

Several studies on the kinetics and mechanism of the thermal unimolecular decomposition of monomethylsilane (MMS) are documented in the literature; yet, to date, the reader is confronted by a number of puzzling discrepancies in the reported data and conclusions. This can be readily visualized from the following chronological summary of findings.

Kohanek, Estacio, and Ring (KER)[1] carried out the flow thermolysis of MMS at 520 °C and found the products to be H_2, 1,2-dimethyldisilane (DMDS), and dimethylsilane (DMS) along with a small amount of CH_4, in relative ratios of 1.0, 0.6, 0.2, and ~0.02, respectively. One year later, in 1970, Ring, Puentes, and O'Neal (RPO)[2] reported that the hydrogen fraction from the flow thermolysis of a mixture of MMS and MMS-d_3 at 510–515 °C and 10–15 Torr consisted of 28.32% D_2, 16.21% HD, and 51–52% H_2. From these and similar results using SiH_4/SiD_4 mixtures they concluded that the two primary processes initiating the decomposition of MMS are

$$CH_3SiH_3 \rightarrow CH_3\ddot{S}iH + H_2 \tag{1a}$$

$$CH_3SiH_3 \rightarrow CH_3SiH_2^\bullet + H^\bullet \tag{1b}$$

At the same time, Davidson[3] carried out some experiments in a static system at 527–627 °C and suggested that Si–C cleavage was also taking place:

$$CH_3SiH_3 \rightarrow CH_3^\bullet + SiH_3^\bullet \tag{1c}$$

As part of our ongoing research program on the thermal and photochemical behavior of silicon hydrides we have examined the static-system thermolysis of MMS in detail and we (NS) reported our preliminary findings in 1978.[4] In brief, the thermolysis of MMS at 40–400 Torr and 340–440 °C generated H_2 and DMDS in approximately equal yields and DMS as a minor (~5%) product under strict conditions of low (<1%) conversion and inert (seasoned) reaction surfaces. CH_4 was not a product. Using C_2H_4 as a radical scavenger, we determined from measurements of H_2 the following Arrhenius parameters for step 1a:

$$\log k_{1a}\ (s^{-1}) = (14.95 \pm 0.11) - (63200 \pm 330)/2.3RT$$

The same coefficients were obtained from the measurement of the DMDS product arising via the reaction

$$CH_3\ddot{S}iH + CH_3SiH_3 \rightarrow (CH_3SiH_2)_2 \tag{2}$$

The radical reaction 1b is probably surface catalyzed and initiates a moderately long chain reaction wherein, in the absence of C_2H_4, large amounts of additional H_2 and DMDS are generated. Thermolysis of MMS-d_3 generated D_2 exclusively.

Subsequently, Davidson and Ring (DR)[5] studied the very low pressure (10^{-1}–10^{-2} Torr) static thermolysis of MMS at 569 and 727 °C using mass spectrometric detection for H_2 and CH_4. The Arrhenius parameters obtained for the decomposition of MMS in the range 625–727 °C

---

† Present address: National Aeronautical Establishment, National Research Council of Canada, Ottawa, Ontario, K1A 0R6, Canada.

[1] Kohanek, J. J.; Estacio, P.; Ring, M. A. *Inorg. Chem.* **1969**, *8*, 2516.

[2] Ring, M. A.; Puentes, M. J.; O'Neal, H. E. *J. Am. Chem. Soc.* **1970**, *92*, 4845.

[3] Davidson, I. M. T. *J. Organomet. Chem.* **1970**, *24*, 97.

[4] Neudorfl, P. S.; Strausz, O. P. *J. Phys. Chem.* **1978**, *82*, 241.

[5] Davidson, I. M. T.; Ring, M. A. *J. Chem. Soc., Faraday Trans. 1* **1980**, *76*, 1520.

0002-7863/87/1509-5780$01.50/0

$$\log k_{1a}\ (\mathrm{s}^{-1}) = (14.1 \pm 0.2) - (64771 \pm 72)/2.3RT$$

are in good agreement with ours. Significantly, the authors noted curvature in the Arrhenius plot below 569 °C and suggested that this was due to the onset of heterogeneous decomposition as the temperature was lowered. While reliable measurements of CH_4 could only be achieved at high temperatures (>657 °C), the authors noted a clear increasing trend in the H_2/CH_4 ratio with decreasing temperature. CH_4 was postulated to arise molecularly from

$$CH_3SiH_3 \rightarrow CH_4 + {:}SiH_2 \qquad (1d)$$

rather than via $CH_3^{\bullet}$ from step 1c.

Recently, Sawrey, O'Neal, and Ring (SOR)[6] reexamined the static-system thermolysis of MMS at 427 °C and 150 Torr. Although extrapolation of the kinetic data of Sawrey, O'Neal, Ring, and Coffey (SORC)[7,8] for the overall decomposition obtained in shock-tube experiments in the range 852–977 °C to 427 °C yielded Arrhenius parameters in good agreement with those obtained by NS and DR, the nature of the reported products and their distribution were very different from those obtained by NS[4] and KER.[1] Thus, in the absence of radical traps the major products were reported to be H_2, SiH_4, and DMS, together with small amounts of CH_4. DMDS was clearly stated *not* to be a product: therefore, in the absence of the DMDS-producing step (2), rather esoteric decay paths for $CH_3\ddot{Si}H$ had to be proposed. SOR also concluded that 1,2-H_2 elimination, step 1e, takes place to a small extent since substantial amounts of HD were generated in the pyrolysis of CH_3SiD_3.

$$CH_3SiH_3 \rightarrow CH_2{=}SiH_2 + H_2 \qquad (1e)$$

The nonobservation of DMDS as a major product by SOR, along with their findings that SiH_4 and DMS are major products (in the absence of radical scavengers) and that HD is generated in the thermolysis of MMS-d_3, is clearly at variance with the earlier work of KER[1] and also with our preliminary results.[4] We believe that our more extensive results, which will now be presented, will help to clarify the mechanism of thermolysis of MMS. In particular, we were able to clearly delineate the molecular and radical chain processes and show how the latter, initiated and terminated in a heterogeneous fashion, are strongly influenced by the nature of the surface and the extent of conversion.

Experimental Section

Apparatus. All experiments were carried out in a conventional grease-free, high-vacuum apparatus that was treated with trimethylchlorosilane in order to prevent surface-catalyzed decomposition of the substrates and/or products.[9] The cylindrical quartz reaction vessel of volume 206.6 cm^3 was enclosed in an aluminum block furnace covered by glass wool and transite, and the entire assembly was fitted into an asbestos box. The furnace was heated by eight 300-W pencil heaters arranged in parallel, powered by an API 2-mode proportional electronic controller. Two iron–constantan thermocouples, connected to a Wheelco Instruments potentiometer, were used to monitor the temperature in the reaction vessel. One was positioned on the outside wall and the other in the center. Temperatures were constant to within ±0.2 °C.

For the investigation of surface effects, the vessel was filled with pieces of quartz tubing, the ends of which were fire polished (V = 153.5 cm^3, S/V = 21 cm^{-1}).

Materials. MMS (Merck, Sharp and Dohme) and MMS-d_3 were found to contain DMS as the major impurity. Therefore they were purified by preparative GC using a Pyrex spiral column, 6 ft × 9 mm i.d., packed with Porapack Q (80–100 mesh). Before use, it was purged by a stream of dried helium at 190 °C for several hours, allowed to cool to room temperature, evacuated to <10^{-5} Torr, and cooled to 0 °C. MMS (600 Torr) was then admitted into the column and the fraction that passed through within 8 min was collected for use. No traces (<0.001%) of DMS could be detected by flame ionization GC.

1,2-Dimethyldisilane (DMDS) was prepared from the Hg($^3P_1$)-sensitized decomposition of MMS[10] and purified on a Porapack Q (50–80 mesh) column, 5 ft × 6 mm i.d., 50–160 °C.

DMS (Peninsular) was repeatedly degassed at 130 °C to remove MMS and C_3H_8. In order to separate trimethylsilane (TMS), DMS was first distilled at 115 °C and then purified on the Porapack Q column as for the case of MMS; the column was operated at 25 °C, the pressure of DMS admitted was 150 Torr, and the fraction eluted in 6 min was collected.

Procedures. After thermolysis, the reaction mixture was passed through two traps at −196 and −210 °C, respectively. The gases noncondensible at −210 °C were measured in a gas buret and analyzed on a molecular sieve 13X (30–60 mesh) column, 6 ft × 6 mm i.d., at 25 °C, employing a thermal conductivity GOW-MAC TR-II-B detector. The remaining mixture was measured in a gas buret, transferred to a Pyrex ampule fitted with a mercury-covered Burrel Silicone rubber seal, and brought to a total pressure of 760 Torr by introducing helium through a gas syringe. The contents were mixed by pumping with the syringe, and several samples (5–100 μL) were withdrawn for analysis on a Hewlett-Packard Model 5750 flame ionization chromatograph using two identical Porapack Q (50–80 mesh) columns, 6 ft × $^1/_4$ in., stainless steel, as reference and analysis columns, with temperature programming between 60 and 165 °C. The detector response was calibrated with authentic samples.

Mass spectra were obtained on Associated Electronic Industries instruments, Models MS 2 and MS 12. Hydrogen isotope ratios were determined on AEI Model MS 2 and MS 10 spectrometers.

Results

The products of the low-temperature (340–440 °C) thermolysis of MMS under static conditions are H_2, DMDS, DMS, and SiH_4. CH_4 was only detected after extremely high conversions. A dark brown polymer deposited on the surface of the reaction vessel was also observed. The nature of the polymer was not examined but a heavy, fresh deposit was found to evolve light gases (H_2, CH_4, C_2 and C_3 hydrocarbons, all the methylated monosilanes). Gas evolution ceased upon thorough evacuation of the heated reaction vessel.

Since the nature of the products, their yields, and their ratios were found to be extremely sensitive to the amount of conversion and nature of the surface, a great deal of effort was expended in order to define those conditions that would ensure reproducible results—namely, carrying out several thermolyses to high conversions in order to completely cover the inner surface of the reaction vessel, followed by evacuation at the reaction temperature.

The results in Table I clearly illustrate the problems associated with this study and will later serve to explain, at least partly, the apparently contradictory results reported by other workers.

The effects of increasing conversion are seen for cases A and B: above 1%, the rates of formation of H_2 and DMS increase, while those for DMDS decrease, reflecting the lower thermal stability of DMDS. It appears as though DMS is a product of the thermolysis of DMDS. SiH_4 could be detected at higher conversions, but in erratic and very small yields. The H_2/DMS and DMDS/DMS ratios are even more drastically affected, declining from 24 and 20 to 5.5 and 0.3, respectively, at 20.5% conversion. In this experiment, quite a few additional products were formed but not identified. It should be noted that the extents of conversion were calculated on the basis of the H_2 yields and are therefore minimum values; even so, the old axiom that primary reactions can only be elucidated from low-conversion experiments appears to impose even more severe constraints for the case of MMS.

Increasing the surface to volume ratio 21-fold led to a ~50% increase in the product rates, suggesting the occurrence of minor heterogeneous processes in the unpacked reaction cell.

The effects of surface activity are also illustrated in Table I for case C. Prior to this series of experiments, a packed vessel (S/V = 21 cm^{-1}) was coated with a silicon mirror by heating 100 Torr of SiH_4 at 490 °C for 48 h and then evacuated. Subsequently, between 65.6 and 73.3 Torr of MMS was thermolyzed for 10 min in the sequential order in which the results of Table

---

[6] Sawrey, B. A.; O'Neal, H. E.; Ring, M. A. *Int. J. Chem. Kinet.* **1984**, *16*, 23.

[7] Sawrey, B. A.; O'Neal, H. E.; Ring, M. A.; Coffey, D., Jr. *Int. J. Chem. Kinet.* **1984**, *16*, 7.

[8] Sawrey, B. A.; O'Neal, H. E.; Ring, M. A.; Coffey, D., Jr. *Int. J. Chem. Kinet.* **1984**, *16*, 31.

[9] Purnell, J. H.; Walsh, R. *Proc. R. Soc. London, Ser. A* **1966**, *293*, 543.

[10] Nay, M. A.; Woodall, G. N. C.; Strausz, O. P.; Gunning, H. E. *J. Am. Chem. Soc.* **1965**, *87*, 179.

Table I. Surface and Time Effects on the Product Rates and Distribution

	product rates, μmol min^{-1}				time, min	product ratios			% conversion[a]
	H_2	DMDS	DMS	SiH_4		H_2	DMDS	DMS	
case A[b]	7.27	6.10	0.30	trace	3.0	24	20	1.0	0.37
	7.48	nd[c]	nd	trace	4.0				0.49
	7.28	6.27	0.33	trace	6.0	24	21	1.0	0.69
	7.75	6.31	0.70	0.23	12.0	13	12	1.0	1.32
	6.72	6.08	0.47	0.02	12.0	11	9.0	1.0	1.51
	7.71	5.87	0.84	0.07	18.0	9.6	7.3	1.0	1.77
	8.14	4.81	1.2	0.04	24.0	6.8	4.0	1.0	3.32
case B[d]	4.19×10^{-4}	0.25×10^{-4}	0.76×10^{-4}	0.08×10^{-4}	4750	5.5	0.3	1.0	20.5
case C[e]	9.90	3.69	3.30	1.66	10	3.0	1.1	1.0	0.1–0.5%
	5.82	3.70	2.06	0.85	10	2.8	1.8	1.0	
	3.94	2.80	0.81	nd	10	4.9	3.5	1.0	
	nd	2.62	0.50	nd	10	nd	5.2	1.0	
	2.61	2.31	0.36	0.20	10	7.3	6.4	1.0	
	2.82	2.47	0.43	0.15	10	6.6	5.7	1.0	
	⋮	⋮	⋮	⋮		⋮	⋮	⋮	
	1.86[f]	1.76[f]	0.08[f]	<0.02[f]	10[f]	23[f]	22[f]	1.0[f]	

[a] Based on the H_2 yields. [b] Case A: 124–130 Torr of MMS, 422 °C. "Seasoned" vessel. [c] Not determined. [d] Case B: 88 Torr of MMS, 360 °C. "Seasoned" vessel. CH_4 ($R = 3 \times 10^{-4}$ mol min^{-1}) was also detected. [e] Case C: 60–70 Torr of MMS, 415 °C. Packed vessel ($S/V = 21$ cm^{-1}) freshly coated with a silicon mirror. [f] After careful seasoning.

I are presented. Upon repeated thermolysis, it is seen that the rates of formation of all the products diminish appreciably, those for H_2, DMS, and SiH_4 being the most severely affected. The product ratios also show large variations, those obtained in the "fresh" reaction vessel being comparable to the product ratios obtained at high conversion (case B). For comparison, the product rates and ratios obtained after carefully seasoning the vessel are also included in Table I. It appears that some heterogeneous processes are involved in the thermolysis of MMS and that the polymer is able to deactivate the surface to a high extent. In particular, the results suggest that most, if not all, of the SiH_4 and DMS is formed in a surface-catalyzed reaction.

The results that follow were all obtained from very low conversion (0.2–0.6%, based on the H_2 yields) experiments carried out in a well-seasoned vessel, brought about by repeated (5–10) thermolysis of 70 Torr of MMS at 415 °C for 10 min. Under these conditions, H_2 and DMDS are the sole major products, formed in a ratio of 1.15 ± 0.10, and DMS is a minor product, comprising only 5% of the major products. Table II lists the total H_2 yields obtained at various pressures and temperatures, along with the molecular H_2 yields determined from ethylene-inhibited reactions as well as their differences, attributed to radical H_2 yields initiated by H-atom abstraction (vide infra). Table III lists the H_2, DMDS, and DMS yields at 415 °C and 45–400 Torr.

Reaction orders for the formation of H_2 in the temperature range 341–441 °C were determined from the data in Tables II and III and from the data on the ethylene-inhibited reaction, to be presented in Table V, and are summarized in Table IV. In spite of the scatter, an increasing trend with decreasing temperature is apparent for the order of formation of H_2 in the uninhibited reaction.

In order to delineate the molecular and free radical primary steps, a number of experiments were carried out in the presence of C_2H_4 as a radical scavenger. Addition of C_2H_4 has a profound effect on the product yields, as shown in Figure 1: the H_2 and DMDS yields decrease very rapidly up to 5% added C_2H_4, after which they are constant, DMS is completely suppressed, and some additional products are formed, the most prominent one of which was identified as methylethylsilane (MES) on the basis of its mass spectrum. Moreover, it was observed that in the level-off regions the rates of formation of H_2 and DMDS were highly reproducible (30% of those in the absence of C_2H_4) and not dependent on the nature of the reaction vessel. Although it seems reasonable to conclude that under these conditions the H_2 and DMDS produced in the thermolysis of MMS are of molecular, homogeneous origin, it will be shown that a small fraction of the H_2 (~10%) comes from radical reactions.

Table V summarizes the results obtained from 20 experiments on thermolysis of 38–406 Torr of MMS in the presence of 10% C_2H_4 in the temperature range 340–449 °C. From these data, the orders of formation of H_2 and DMDS, Table IV, were found to be unity (with the exception of the data for H_2 at 340 °C, for which only two measurements were taken).

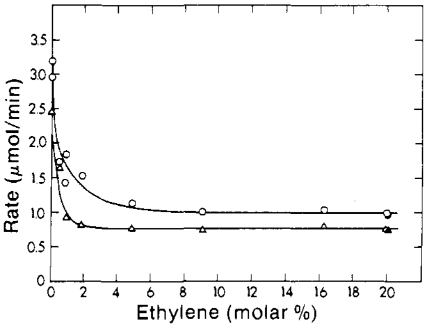

Figure 1. Effect of added ethylene on the rates of product formation in the thermolysis of ~405 Torr of MMS at 415 °C: (○) H_2; (△) DMDS.

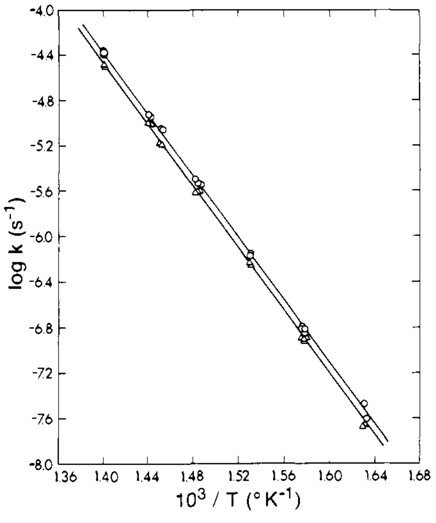

Figure 2. Arrhenius plots for H_2 (○) and DMDS (△) formation from the thermolysis of MMS in the presence of ~10% ethylene.

The Arrhenius plots for H_2 and DMDS formation are shown in Figure 2, from which

$$\log k_{H_2}\ (s^{-1}) = (15.02 \pm 0.10) - (63270 \pm 310)/2.3RT$$

and

$$\log k_{DMDS}\ (s^{-1}) = (14.87 \pm 0.12) - (63150 \pm 350)/2.3RT$$

k_{H_2} is slightly greater than k_{DMDS} because of the unsuppressable radical contribution to the H_2 yield (vide infra). Therefore the Arrhenius parameters obtained for k_{DMDS} more accurately represent the molecular primary step.

Finally, MMS-d_3 (97.0 ± 0.5%) was thermolyzed both in the presence and in the absence of C_2H_4. The results, Table VI, indicate that, within experimental error, hydrogen is formed solely by the cleavage of Si–D bonds.

Discussion

Several primary steps can be envisioned for the pyrolysis of MMS:[11,12]

$$CH_3SiH_3 \rightarrow CH_3\ddot{Si}H + H_2 \qquad \Delta H = 60.1 \text{ kcal mol}^{-1} \qquad (1a)$$

$$CH_3SiH_3 \rightarrow CH_3SiH_2^\bullet + H^\bullet \qquad \Delta H = 89.6 \text{ kcal mol}^{-1} \qquad (1b)$$

$$CH_3SiH_3 \rightarrow CH_3^\bullet + SiH_3^\bullet \qquad \Delta H = 87.4 \text{ kcal mol}^{-1} \qquad (1c)$$

$$CH_3SiH_3 \rightarrow CH_4 + {:}SiH_2 \qquad \Delta H = 54.4 \text{ kcal mol}^{-1} \qquad (1d)$$

$$CH_3SiH_3 \rightarrow CH_2{=}SiH_2 + H_2 \qquad \Delta H = 46 \text{ kcal mol}^{-1} \qquad (1e)$$

Formation of molecular H_2 and methylsilylene, step 1a, is expected to be the dominant mode of homogeneous decomposition,[3] and this is generally acknowledged to be the case.

In an early investigation RPO[2] proposed that Si–H cleavage to produce H atoms and methylsilyl radicals, step 1b, also contributes to the overall decomposition but this reaction was not considered at all in the later mechanism proposed by DR[5] and SOR[6] for static conditions, nor by SORC[7,8] for shock-tube conditions, presumably because of its high-energy requirements. We shall show, however, that step 1b occurs to a small extent, initiating a radical chain in the uninhibited reaction; it is at least partly, if not entirely, heterogeneous and therefore E_{1b} is substantially less than the thermochemically predicted value.

The occurrence of C–Si cleavage, step 1c, has similarly been discounted on thermochemical grounds.[5] The results in Table I (case C) suggest that it may occur in the presence of highly active surfaces.

KER[1] reported CH_4 to be a product of the flow thermolysis of MMS at 520 °C but in very low yields, ~2% of the H_2. Although they did not indicate the extent of conversion in this experiment, the product yields are quoted in mmol units; hence it must have been very high. We observed a similar yield of CH_4 at the highest conversion attempted (20%, Table I) but could not detect it as a product the low-conversion experiments. Nor could we positively detect any methyldisilane, which would have been formed via insertion of $:SiH_2$ into the substrate. DR[5] detected small but measurable amounts of CH_4 in the temperature range 569–727 °C and also observed that the H_2/CH_4 ratio increased with decreasing temperature. They estimated that $E_{1d} - E_{1a} \simeq$ 4 kcal mol^{-1} and that in the temperature range 340–440 °C the H_2/CH_4 ratio would vary between 89 and 56. SOR[6] however, while acknowledging that CH_4 production is a minor reaction channel, claim that it occurs to a slightly greater extent than predicted by DR.[5] Nevertheless, in the low-temperature and low-conversion regimes employed in the present investigation, step 1d can be reasonably excluded from the mechanism.

1,2-Hydrogen elimination, step 1e, would be reflected in the yield of HD from the thermolysis of CH_3SiD_3, as observed by SOR.[6] At this point we would like to reiterate our earlier observation[13] that the extent of isotopic mixing taking place during the thermolysis of silanes strongly depends on the previous history of the reaction vessel. Thus, if the thermolysis of CH_3SiH_3 is carried out immediately following thermolysis of CH_3SiD_3, measurable amounts of D_2 and HD are formed. Especially pertinent are the results of Bradshaw et al.,[14] who observed isotopically mixed hydrogen from CH_3SiD_3 and exchange reactions between CH_3SiH_3 and CH_3SiD_3, and CH_3SiH_3 and D_2, when the methylsilanes were chemisorbed on nickel, rhodium, or tungsten surfaces at −78 and +20 °C. In view of these observations and also because active surfaces promote radical chain hydrogen formation (Table I), the experiments reported in Table VI were carried out in a vessel that had been carefully seasoned by the repeated thermolysis of CH_3SiD_3. As an additional precaution the conversions were kept minimal in order to avoid complications from secondary reactions. As can be seen, there is no evidence for C–H cleavage.

Therefore, under conditions of low conversion and inert reactor surfaces, the only important primary processes are steps 1a and 1b, which generate molecular and atomic hydrogen, respectively. The mechanistic sequence we propose for the thermolysis of MMS is outlined in Table VII. The other major product, DMDS, can be formed by insertion of methylsilylene into the Si–H bond of the substrate, step 2, or from $CH_3SiH_2^\bullet$ precursors, steps 4 and 5. The exact mechanistic pathway leading to the formation of the minor product DMS is, as we shall see, less obvious.

We shall first consider the mechanism of the inhibited reaction and then delineate the radical processes.

Molecular Processes. In the presence of C_2H_4, *both* the H_2 and DMDS yields are strongly suppressed while DMS is no longer a product. Thus a large fraction of the H_2 and DMDS products and all the DMS found in the thermolysis of neat MMS come from free radical precursors, and these can only be $H^\bullet$ and $CH_3SiH_2^\bullet$ generated in (1b). In the presence of 10% C_2H_4, the competing processes are

$$H^\bullet + CH_3SiH_3 \rightarrow H_2 + CH_3SiH_2^\bullet \qquad (3)$$

$$H^\bullet + C_2H_4 \rightarrow C_2H_5^\bullet \qquad (8)$$

for $H^\bullet$ atoms,

$$CH_3SiH_2^\bullet + CH_3SiH_3 \rightarrow DMDS + H^\bullet \qquad (4)$$

$$2CH_3SiH_2^\bullet \rightarrow DMDS \qquad (5)$$

$$CH_3SiH_2^\bullet + C_2H_4 \rightarrow CH_3SiH_2CH_2CH_2^\bullet \qquad (9)$$

for $CH_3SiH_2^\bullet$ radicals, and

$$CH_3\ddot{Si}H + CH_3SiH_3 \rightarrow DMDS \qquad (2)$$

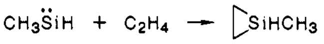
$CH_3\ddot{Si}H + C_2H_4 \rightarrow$ SiHCH$_3$ (10)

for CH_3SiH:. Since $CH_3SiH_2CH_2CH_2^\bullet$ is an efficient hydrogen abstractor, C_2H_4 generates a chain reaction in $CH_3SiH_2^\bullet$ (Table VII).

Arrhenius parameters for the $H^\bullet$-atom reactions with MMS[16] and C_2H_4[17] are identical, within experimental error, and thus, for a mixture containing 10% C_2H_4, $R_8/R_3 \simeq 0.11$. This simple calculation, however, refers only to the trapping efficiency of C_2H_4 relative to H abstraction from the substrate and shows that the latter reaction cannot be suppressed under the conditions employed. From Figure 1, however, it is seen that only ~1% C_2H_4 effects a ~50% reduction in R_{H_2}, and even above ~20% C_2H_4, R_{H_2} remains constant at only ~30% of its initial value. It is obvious, then, that the high efficiency of C_2H_4 in suppressing R_{H_2} is not due to the scavenging of $H^\bullet$ atoms produced in the initial reaction but rather to the rapid scavenging of some radical that generates $H^\bullet$ atoms in a chain propagation step. The only radical produced in a primary process, which can be efficiently trapped by C_2H_4, is $CH_3SiH_2^\bullet$ and therefore we propose displacement reaction 4 as an additional source of $H^\bullet$ atoms.

Similar arguments require that in the uninhibited reaction, most of the DMDS be also produced in a chain process, and displacement reaction 4 satisfies this condition as well. Note that recombination of $CH_3SiH_2^\bullet$ radicals, step 5, is a chain termination

---

(11) $\Delta H_f(CH_3SiH:) = 51.9$ kcal mol^{-1}; vide infra.

(12) $\Delta H_f(CH_3SiH_3) = -7$, $\Delta H_f(CH_3SiH_2^\bullet) = 30.5$, $\Delta H_f(SiH_3^\bullet) = 46.4$, $\Delta H_f(CH_2{=}SiH_2) = 39 \pm 5$ kcal mol^{-1}: Walsh, R. *Acc. Chem. Res.* **1981**, *14*, 246; $\Delta H_f(SiH_2:) = 65.3 \pm 1.5$ kcal mol^{-1}: Frey, H. M.; Walsh, R.; Watts, I. M. *J. Chem. Soc., Chem. Commun.* **1986**, 1189.

(13) Neudorfl, P.; Jodhan, A.; Strausz, O. P. *J. Phys. Chem.* **1980**, *84*, 338.

(14) Bradshaw, D. I.; Moyes, R. B.; Wells, P. B. *J. Chem. Soc., Faraday Trans. 1* **1980**, *76*, 979.

(15) Atwell, W. A.; Weyenberg, D. R. *Angew. Chem., Int. Ed. Engl.* **1969**, *8*, 469.

(16) Arthur, N. L.; Bell, T. N. *Rev. Chem. Intermed.* **1978**, *2*, 37.

(17) Lee, J. H.; Michael, J. V.; Payne, W. A.; Stief, L. J. *J. Chem. Phys.* **1978**, *68*, 1817.

Table II. Hydrogen Yields from the Thermolysis of MMS as a Function of Pressure and Temperature

P(MMS), Torr	time, s	H_2 yield, μmol			rate, M s^{-1}		
		tot	mol[a]	rad[b]	H_2(tot)	H_2(mol)	H_2(rad)
T = 441 °C							
171.5	60.6	2.47	1.67	0.80	1.98×10^{-7}	1.34×10^{-7}	6.44×10^{-8}
118.0	60	1.57	1.14	0.43	1.27×10^{-7}	0.92×10^{-7}	3.51×10^{-8}
80.8	60.6	1.05	0.78	0.27	0.84×10^{-7}	0.63×10^{-7}	2.12×10^{-8}
57.6	90	1.11	0.83	0.28	0.60×10^{-7}	0.45×10^{-7}	1.50×10^{-8}
39.5	120	1.02	0.76	0.26	0.41×10^{-7}	0.31×10^{-7}	1.05×10^{-8}
T = 429 °C							
203.5	90	2.97	1.40	1.57	1.60×10^{-7}	0.75×10^{-7}	0.85×10^{-8}
138.2	90	1.76	0.95	0.81	0.94×10^{-7}	0.51×10^{-7}	0.43×10^{-8}
94.0	120	1.38	0.86	0.52	0.56×10^{-7}	0.35×10^{-7}	0.21×10^{-8}
63.7	180	1.41	0.87	0.54	0.38×10^{-7}	0.24×10^{-7}	0.14×10^{-8}
42.8	240	1.24	0.78	0.46	0.25×10^{-7}	0.16×10^{-7}	0.09×10^{-8}
T = 421 °C							
214.3	150	2.34	1.50	0.84	7.55×10^{-8}	4.84×10^{-8}	2.72×10^{-8}
177.0	150	1.87	1.23	0.64	6.03×10^{-8}	4.00×10^{-8}	2.03×10^{-8}
147.1	150	1.53	1.03	0.50	4.94×10^{-8}	3.32×10^{-8}	1.62×10^{-8}
125.7	192	1.66	1.12	0.54	4.19×10^{-8}	2.84×10^{-8}	1.35×10^{-8}
120.2	180	1.48	1.01	0.47	3.98×10^{-8}	2.71×10^{-8}	1.27×10^{-8}
100.3	183	1.21	0.85	0.36	3.20×10^{-8}	2.26×10^{-8}	0.94×10^{-8}
81.4	270	1.44	1.02	0.42	2.58×10^{-8}	1.83×10^{-8}	0.75×10^{-8}
69.2	270	1.18	0.87	0.31	2.11×10^{-8}	1.56×10^{-8}	0.55×10^{-8}
55.7	360	1.26	0.93	0.33	1.69×10^{-8}	1.25×10^{-8}	0.44×10^{-8}
47.1	390	1.18	0.85	0.33	1.47×10^{-8}	1.06×10^{-8}	0.41×10^{-8}
31.6	540	1.05	0.79	0.26	0.94×10^{-8}	0.70×10^{-8}	0.24×10^{-8}
T = 400 °C							
212.3	360	1.84	0.86	0.98	2.48×10^{-8}	1.16×10^{-8}	1.32×10^{-8}
209.0	360	1.50	0.85	0.65	2.02×10^{-8}	1.14×10^{-8}	0.88×10^{-8}
202.9	600	2.75	1.37	1.38	2.22×10^{-8}	1.11×10^{-8}	1.11×10^{-8}
148.5	600	1.85	1.00	0.85	1.49×10^{-8}	0.81×10^{-8}	0.68×10^{-8}
144.4	600	1.73	0.97	0.76	1.40×10^{-8}	0.79×10^{-8}	0.61×10^{-8}
138.6	660	1.81	1.03	0.78	1.33×10^{-8}	0.76×10^{-8}	0.57×10^{-8}
135.8	426	1.19	0.65	0.54	1.36×10^{-8}	0.74×10^{-8}	0.62×10^{-8}
93.9	600	1.09	0.63	0.46	0.88×10^{-8}	0.51×10^{-8}	0.37×10^{-8}
91.8	600	0.99	0.62	0.37	0.80×10^{-8}	0.50×10^{-8}	0.30×10^{-8}
73.7	900	1.22	0.75	0.47	0.66×10^{-8}	0.40×10^{-8}	0.26×10^{-8}
62.9	918	1.03	0.65	0.38	0.54×10^{-8}	0.34×10^{-8}	0.20×10^{-8}
61.9	780	0.84	0.54	0.30	0.52×10^{-8}	0.33×10^{-8}	0.19×10^{-8}
48.5	900	0.80	0.49	0.31	0.43×10^{-8}	0.26×10^{-8}	0.17×10^{-8}
42.3	1200	0.87	0.57	0.30	0.35×10^{-8}	0.23×10^{-8}	0.12×10^{-8}
33.7	1440	0.80	0.55	0.35	0.27×10^{-8}	0.18×10^{-8}	0.09×10^{-8}
T = 380 °C							
212.8	990	1.58	0.59	0.99	7.73×10^{-9}	2.87×10^{-9}	4.86×10^{-9}
210.2	660	1.09	0.39	0.70	7.99×10^{-9}	2.84×10^{-9}	5.15×10^{-9}
145.2	1290	1.15	0.52	0.63	4.32×10^{-9}	1.96×10^{-9}	2.36×10^{-9}
141.5	1560	1.34	0.61	0.73	4.16×10^{-9}	1.91×10^{-9}	2.25×10^{-9}
96.5	1800	0.94	0.48	0.46	2.53×10^{-9}	1.30×10^{-9}	1.23×10^{-9}
65.2	1860	0.60	0.34	0.26	1.57×10^{-9}	0.88×10^{-9}	0.69×10^{-9}
42.9	2820	0.57	0.34	0.23	0.98×10^{-9}	0.58×10^{-9}	0.40×10^{-9}
T = 361 °C							
92.6	8880	1.26	0.54	0.72	6.87×10^{-10}	2.94×10^{-10}	3.93×10^{-10}
62.1	12600	1.03	0.51	0.52	3.95×10^{-10}	1.97×10^{-10}	1.98×10^{-10}
40.5	16800	0.85	0.45	0.40	2.45×10^{-10}	1.28×10^{-10}	1.17×10^{-10}
T = 341 °C							
195.8	16500	2.32	0.43	1.89	6.81×10^{-10}	1.25×10^{-10}	5.56×10^{-10}
128.2	19500	1.34	0.33	1.01	3.32×10^{-10}	0.82×10^{-10}	2.50×10^{-10}
84.5	33180	1.19	0.37	0.82	1.73×10^{-10}	0.54×10^{-10}	1.19×10^{-10}

[a] Calculated from the Arrhenius expression log $k = 14.87 - 63150/2.3RT$. [b] From H_2(tot) − H_2(mol).

reaction and therefore should not make a significant contribution to the total DMDS yields. Unfortunately, the kinetic parameters for reactions 4 and 9 have not been reported; however, we can arrive at some reasonable estimates.

Since $D(CH_3SiH_2{-}H) = 89.6$ kcal mol^{-1} and $D(CH_3SiH_2{-}H_2SiCH_3) \sim 76$ kcal mol^{-1},[12] reaction 4 will be endothermic by $\sim$14 kcal mol^{-1}. For the $H^{\bullet} + Si_2H_6 \rightarrow SiH_3^{\bullet} + SiH_4$ reaction the activation energies for the forward[18] and reverse[2] reactions have been estimated to be $\sim$3 and $\sim$15 kcal mol^{-1}, respectively. Hence E_4 should be approximately 17 kcal mol^{-1}. Assuming $A_4 \sim 10^9$ M^{-1} s^{-1},[19] then at 400 °C $k_4 < 3 \times 10^4$ M^{-1} s^{-1}.

The only rate constant data that have been reported for the addition of a silicon-centered radical to C_2H_4 are for the cases of $SiD_3SiD_2^{\bullet}$,[18] $(CH_3)_3Si^{\bullet}$,[20] and $(C_2H_5)_3Si^{\bullet}$.[21] For $SiD_3SiD_2^{\bullet}$, $k_{add}^{298} \sim 4 \times 10^6$ M^{-1} s^{-1}; for $(CH_3)_3Si^{\bullet}$, $k_{add}^{298} \sim (1.7 \pm 1.0) \times 10^5$ M^{-1} s^{-1} with log A (M^{-1} s^{-1}) = 7.0 ± 0.02 and E_a = 2.5

---

(18) Pollock, T. L.; Sandhu, H. S.; Jodhan, A.; Strausz, O. P. *J. Am. Chem. Soc.* **1973**, *95*, 1017.

(19) Benson, S. W. *Thermochemical Kinetics*, 2nd ed.; Wiley: New York, 1976.

(20) Choo, K. Y.; Gaspar, P. P. *J. Am. Chem. Soc.* **1974**, *96*, 1284.

(21) Chatgilialoglu, C.; Ingold, K. U.; Scaiano, J. C. *J. Am. Chem. Soc.* **1983**, *105*, 3292.

Table III. H_2, DMDS, and DMS Yields as a Function of Pressure at 415 °C

P(MMS), Torr	time, s	H_2 yield, μmol			DMDS yield, μmol			DMS yield, μmol	rate, M s^{-1}					
		tot	mol[a]	rad[b]	tot	mol[a]	rad[b]		$10^8R_{H_2}^{tot}$	$10^8R_{H_2}^{mol\ c}$	$10^8R_{H_2}^{rad}$	$10^8R_{DMDS}^{tot}$	$10^8R_{DMDS}^{rad}$	10^9R_{DMS}
400.7	120	3.63	1.49	2.14	3.20	1.49	1.71	0.10	14.6	6.03	8.57	12.9	6.87	4.03
404.8	120	3.46	1.51	1.95	2.76	1.51	1.25	0.074	14.0	6.09	7.90	11.1	5.02	2.99
407.8	120	3.03	1.52	1.51	2.76	1.52	1.24	0.060	12.2	6.14	6.07	11.1	4.96	2.42
241.5	150	1.98	1.13	0.85	1.85	1.13	0.72	0.052	6.39	3.63	2.75	5.97	2.34	1.68
198.5	120	1.58	0.74	0.84	1.33	0.74	0.59	0.046	6.37	2.99	3.39	5.38	2.38	1.86
154.8	150	1.31	0.72	0.59	0.95	0.72	0.23	0.023	4.23	2.33	1.90	3.07	0.74	0.74
138.5	150	1.15	0.65	0.50	0.78	0.65	0.13	0.022	3.72	2.08	1.62	2.52	0.43	0.71
144.2	720	4.93	3.23	1.70	4.23	3.23	1.00	0.090	3.32	2.17	1.14	2.84	0.67	0.61
109.1	150	0.80	0.51	0.29	0.66	0.51	0.15	0.010	2.58	1.64	0.93	2.13	0.49	0.32
49.3	150	0.32	0.23	0.09	0.42	0.23	0.19	0.004	1.03	0.74	0.29	1.36	0.62	0.13
48.9	180				0.38	0.27	0.11	0.004		0.73		1.02	0.30	0.11
45.4	180	0.36	0.25	0.11	0.31	0.25	0.06	0.004	0.97	0.68	0.30	0.83	0.16	0.11

[a] Calculated from the Arrhenius expression $\log k = 14.87 - 63150/2.3RT$. [b] From X(tot) − X(mol). [c] $R_{H_2}^{mol} \simeq R_{DMDS}^{mol}$.

Table IV. Reaction Orders for Hydrogen and Dimethyldisilane Formation

T, °C	H_2(tot)[a]	H_2(rad)[a]	H_2(mol)[b]	DMDS(mol)[b]
441	1.06 ± 0.03	2.02 ± 0.41	1.02 ± 0.01	1.00 ± 0.01
429	1.19 ± 0.05	1.73 ± 0.19		
421	1.09 ± 0.01	2.03 ± 0.10	1.03[c]	0.99[c]
415	1.22 ± 0.04	1.82 ± 0.23	1.00 ± 0.01	0.97 ± 0.04
400	1.16 ± 0.02	1.72 ± 0.08	1.06 ± 0.04	0.97 ± 0.05
380	1.31 ± 0.04	1.82 ± 0.07	0.95[c]	1.03[c]
361	1.24 ± 0.07	1.66 ± 0.17	1.00 ± 0.01	1.02 ± 0.01
341	1.63 ± 0.04	1.92 ± 0.02	1.25[c]	0.93[c]

[a] From the data in Tables II and III. [b] From the data in Table V. [c] Only two experiments were done.

± 0.2 kcal mol^{-1}; for $(C_2H_5)_3Si^•$, $k_{add}^{298} = (2.2 \pm 0.4) \times 10^7$ M^{-1} s^{-1} with $\log A$ (M^{-1} s^{-1}) = 8.40 ± 0.60 and E_a = 1.40 ± 0.80 kcal mol^{-1}. The kinetic data for the disilyl radical are not, however, necessarily comparable with those for alkylsilyl radicals. The rate constant reported by Choo and Gaspar[20] for addition of $(CH_3)_3Si^•$ radicals to C_2H_4 appears to be too low, as has been recently pointed out by Chatgilialoglu, Ingold, and Scaiano.[21] We believe that the rate parameters for reaction 9 should be very similar to those reported for the $(C_2H_5)_3Si^• + C_2H_4$ reaction[21] and therefore we estimate that at 400 °C $k_9 \sim 3.5 \times 10^7$ M^{-1} s^{-1}. Thus, in the presence of 10% C_2H_4, $R_9/R_4 \sim 130$ at 400 °C and the chain cannot be sustained.

With regard to the methylsilylene radicals generated in the primary molecular process (1a), we now have to evaluate the relative rates of insertion, (2), and addition to C_2H_4, (10). On the basis of relative rate measurements, Davidson et al.[22] concluded that insertion of $(CH_3)_2Si$: into Si–H bonds proceeds with zero activation energy. Recently, the absolute rate constants for insertion of SiH_2: into Si_2H_6 and addition of SiH_2: to C_2H_4 have been determined[23] to be 3.43×10^{11} and 5.84×10^{10} M^{-1} s^{-1}, respectively. These values are close to collision frequencies and should be reasonable approximations for the values of k_2 and k_{10}. With the assumption $E_2 = E_{10} = 0$, then for 10% C_2H_4 $R_2/R_{10} \simeq 53$ and thus scavenging of CH_3SiH: by C_2H_4 is not important under these conditions. It should also be noted that the rate constant for insertion of SiH_2: into CH_4 is much smaller, 6.0 ×

Table V. The MMS–C_2H_4 System: Yields of H_2 and DMDS as a Function of MMS Pressure, Time, and Temperature

T, °C	P(MMS), Torr	time, min	$[C_2H_4]/[MMS]$	H_2, μmol	DMDS, μmol	k_{1b},[a] s^{-1}	k_{DMDS}, s^{-1}
440	278.3	2.50	0.111	8.17	6.24	1.11×10^{-5}	3.22×10^{-5}
441	133.4	2.50	0.107	3.95	3.03	1.10×10^{-5}	3.26×10^{-5}
440	43.0	2.50	0.107	1.22	0.96	9.60×10^{-6}	3.21×10^{-5}
421	282.3	3.00	0.107	2.87	2.25	2.83×10^{-6}	9.28×10^{-6}
420	62.7	6.50	0.107	1.33	1.10	2.18×10^{-6}	9.42×10^{-6}
415	404.6	2.50	0.100	2.53	1.84	2.60×10^{-6}	6.40×10^{-6}
415	277.9	2.50	0.195	1.75	1.31	2.62×10^{-6}	6.53×10^{-6}
415	194.9	2.50	0.195	1.21	0.91	2.55×10^{-6}	6.46×10^{-6}
415	58.4	10.00	5.554	1.46	nd[b]		
401	406.3	4.00	0.107	1.50	1.14	8.32×10^{-7}	2.38×10^{-6}
399	192.7	8.00	0.111	1.30	1.18	2.92×10^{-7}	2.59×10^{-6}
400	90.9	16.00	0.107	1.23	1.07	4.12×10^{-7}	2.49×10^{-6}
380	189.3	30.00	0.107	1.17	1.00	1.09×10^{-7}	5.78×10^{-7}
380	57.3	125.00	0.111	1.57	1.21[c]	1.84×10^{-7}	5.56×10^{-7}
360	278.2	100.0	0.166	1.34	1.09	3.34×10^{-8}	1.25×10^{-7}
360	280.7	100.0	0.110	1.36	1.08	3.53×10^{-8}	1.23×10^{-7}
360	84.6	340.0	0.111	1.35	1.05	3.69×10^{-8}	1.16×10^{-7}
361	38.1	792.0	0.111	1.48	1.13	4.11×10^{-8}	1.19×10^{-7}
340	398.4	370.0	0.111	1.55	1.00	1.28×10^{-8}	2.09×10^{-8}
340	127.6	910.0	0.111	0.92	0.85	2.07×10^{-9}	2.26×10^{-8}

[a] Calculated from: $R_{1b} = (R_{H_2} - R_{DMDS})(1 + [C_2H_4]/[MMS])$. The second term is a correction for the $H^•$ atoms trapped by C_2H_4. [b] Not determined. [c] Traces of DMS present.

Table VI. Isotopic Distribution of Hydrogen from the Thermolysis of MMS-d_3

T, °C	P(MMS-d_3), Torr	time, min	H_2, μmol	molar %		
				H_2	HD	D_2
401[a]	370.1	12.75	2.44	0.58	4.68	94.74
403[a]	284.5	20.00	2.52	0.45	4.51	95.04
415[a]	193.1	18.00	4.70	0.43	4.41	95.17
401	364.2	12.00	4.94	0.7	2.1	97.2
401	251.7	12.00	3.27	1.82	1.95	96.23

[a] In the presence of 9.90% added ethylene.

Scheme I

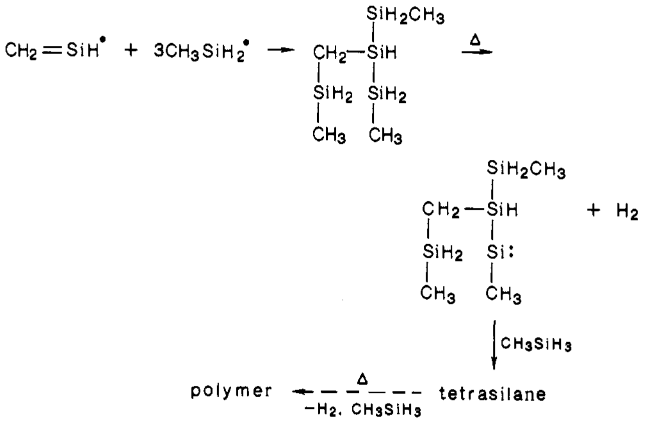

10^8 M^{-1} s^{-1}, and consequently insertion of $CH_3\ddot{S}iH$ into the C–H bonds of MMS can be considered to be negligible.

The H_2/DMDS ratios averaged 1.15 ± 0.10 in the neat thermolyses and 1.27 ± 0.10 in the presence of C_2H_4. We believe that the deficiency in DMDS in the unscavenged reaction is due to slow secondary thermolysis of the $CH_3SiH_2^\bullet$ radical, e.g., $CH_3SiH_2^\bullet \xrightarrow{\Delta} CH_2{=}SiH^\bullet + H_2$, which can compete with the other DMDS-producing reaction, step 4. The $CH_2{=}SiH^\bullet$ species can then scavenge three $CH_3SiH_2^\bullet$ radicals to generate a tetrasilane having three adjacent silicon atoms: this configuration is thermally unstable and the polysilane should decompose readily with loss of H_2 to form a high molecular weight silylene, which ultimately ends up as a polymer (Scheme I). Of course, one can envisage a number of alternative schemes resulting in loss of $CH_3SiH_2^\bullet$ and production of excess H_2 and polymers. In the C_2H_4-inhibited reaction, on the other hand, the higher H_2/DMDS ratio is due to a contribution to the H_2 yields from the primary radical step (1b) followed by abstraction, (3), since—as was shown above—step 3 cannot be suppressed by only 10% C_2H_4. Thus from Figure 1, $k_{1b} = 1.7 \times 10^{-6}$ M^{-1} s^{-1} at 415 °C, compared with the value 3.1×10^{-7} M^{-1} s^{-1} derived from kinetic treatment of the results (vide infra).

SOR[6] also recognized the presence of free radicals in the thermal decomposition of MMS but suggested that they are generated in two ways: in a surface-catalyzed reaction

$$CH_3SiH{:} + \text{wall} \rightarrow \text{wall}{\sim}CH_3SiH{:}\ (W') \qquad (12)$$

$$CH_3SiH_3 \text{ or } CH_3SiH{:} + W' \rightarrow CH_3SiH_2^\bullet + W'' \qquad (13)$$

and in various reactions involving $CH_3SiH{:}$ as precursor

$$CH_3SiH_2^\bullet + CH_3SiH{:} \rightsquigarrow (CH_3)_2Si{:} + SiH_3^\bullet \qquad (14)$$

$$SiH_3^\bullet + CH_3SiH_3 \rightarrow CH_3SiH_2^\bullet + SiH_4 \qquad (15)$$

$$(CH_3)_2Si{:} + CH_3SiH_3 \rightsquigarrow CH_3SiH{:} + (CH_3)_2SiH_2 \qquad (16)$$

$$CH_3SiH{:} \rightleftarrows CH_2{=}SiH_2 \qquad (17)$$

$$CH_2{=}SiH_2 + CH_3SiH{:} \rightsquigarrow SiH_2{:} + CH_2{=}SiHCH_3 \qquad (18)$$

$$CH_2{=}SiHCH_3 \rightleftarrows (CH_3)_2Si{:} \qquad (19)$$

$$2CH_3SiH{:} \rightleftarrows [CH_3HSi{=}SiHCH_3 \rightleftarrows (CH_3)_2HSi{-}SiH{:} \rightleftarrows (CH_3)_2Si{=}SiH_2] \rightarrow (CH_3)_2Si{:} + SiH_2{:} \qquad (20)$$

(the unstable intermediates formed in steps 14, 16, and 18 are not shown for the sake of simplicity). In the next section we shall clearly demonstrate that the primary generation of $H^\bullet$ and $CH_3SiH_2^\bullet$ is surface catalyzed. SOR's steps 12 and 13 are therefore not in basic agreement with our step 1b but in view of the near equivalence of the H_2 and DMDS yields we do not believe $CH_3SiH{:}$ to be a precursor to $CH_3SiH_2^\bullet$. Moreover, in view of the high rate constant values recently reported[23] for insertion of $:SiH_2$ into Si–H bonds, it is highly unlikely that diffusion-controlled reaction 12 can compete with insertion reaction 2, which is extremely fast at the MMS pressure employed. To our knowledge, step 14 has not been proposed elsewhere in the literature; in any case, we do not believe that radical–radical reactions involving $CH_3SiH{:}$ such as (14) and (20) could compete effectively with the $CH_3SiH{:} + CH_3SiH_3$ reaction. It is also unlikely that the silylene–silaolefin isomerization, step 17, is significant under the conditions of the experiments. Thus, $CH_3SiH{:}$ generated from the high-energy (147 nm) photolysis of MMS, where the excess energy carried by H_2 and $CH_3SiH{:}$ is ~144 kcal, appears to be relatively stable[24] with respect to isomerization or fragmentation. While $CH_3SiH{:}$ and $CH_2{=}SiH_2$ are calculated[25,26] to be nearly isoenergetic, a very high barrier of 43.8 kcal mol^{-1} for the methylsilylene–silaethylene interconversion is predicted[26] from ab initio type SCF-MO-CI calculations. The (reversible) methylsilylene–silaethylene interconversion can be photochemically induced, however.[27]

The fact that DMDS and H_2 are the sole major products of the thermolysis of MMS under carefully controlled conditions, however, obviates the necessity of postulating radical-generating reactions from silylene precursors, and the sole fate of $CH_3SiH{:}$ is rapid insertion into the Si–H bond of the substrate. We are at a loss to explain why DMDS was detected by us and by KER[1] and not by SOR.[6]

The enthalpy change for reaction 1a, $\Delta H_{1a} = 60.1$ kcal mol^{-1}, can be obtained by using the values $\Delta H^\circ_f(CH_3SiH_3) = -7.0$ kcal mol^{-1} [12] and $\Delta H^\circ_f(CH_3SiH{:}) = 53.1$ kcal mol^{-1} [29] from the literature. On the other hand, using the relationship

$$\Delta H_{1a} = E_{1a} - E_{-1a} + \Delta nRT$$

and assuming that E_{-1a} is the same as the value 5.5 kcal mol^{-1} reported for the $SiH_2 + H_2$ reaction,[28] from our measured activation energy we obtain $\Delta H_{1a} = 63.2 - 5.5 + 1.2 = 58.9$ kcal mol^{-1}, from which $\Delta H^\circ_f(CH_3SiH{:}) = 51.9$ kcal mol^{-1}. This value is close to that of 53.1 kcal mol^{-1} estimated earlier[29] from older thermochemical data.

Finally, ΔH_{1a} can also be expressed as

$$\Delta H_{1a} = D(CH_3SiH_2{-}H) + D(CH_3\dot{S}iH{-}H) - D(H{-}H)$$

and using $D(CH_3SiH_2{-}H) = 89.6$ kcal mol^{-1} [12] we obtain, for $D(CH_3\dot{S}iH{-}H)$, 73.5 kcal mol^{-1}.

The A factor for reaction 1a corresponds to an activation entropy $\Delta S^\ddagger_{1a} = 6.3$ eu, suggesting a rather loose transition state. The most probable configuration of the transition state is a three-centered cyclic structure such as

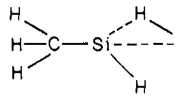

The activation entropy, $\Delta S^\ddagger_{1a} = S^{\circ\ddagger}_{AC} - S^\circ_{MMS}$, can be estimated by Benson's method[19] by using literature values for the fundamental frequencies of MMS,[30] by evaluating the contributions to $S^{\circ\ddagger}_{AC}$ from the specific structural changes in the transition of the MMS molecule into the activated complex.

The rotational contribution comes from the destruction of the threefold symmetry around the C–Si bond, and it is equal to $R \ln 3 = 2.2$ eu. The weakened stretching and bending modes of the Si–H bonds participating in the cyclic structure of the activated complex will give a vibrational contribution of about 3.9 eu, which brings the total to 6.1 eu, close to the value obtained from the A factor.

---

[22] Davidson, I. M. T.; Lawrence, F. T.; Ostah, N. A. *J. Chem. Soc., Chem. Commun.* **1980**, 859.

[23] Inoue, G.; Suzuki, M. *Chem. Phys. Lett.* **1985**, *122*, 361.

[24] Obi, K.; Clement, A.; Gunning, H. E.; Strausz, O. P. *J. Am. Chem. Soc.* **1969**, *91*, 1622.

[25] Schaeffer, H. F., III. *Acc. Chem. Res.* **1982**, *15*, 283.

[26] Goddard, J. D.; Yoshioka, Y.; Schaeffer, H. F., III. *J. Am. Chem. Soc.* **1980**, *102*, 7644.

[27] Reisenauer, H. P.; Mihm, G.; Maier, G. *Angew. Chem., Int. Ed. Engl.* **1982**, *21*, 854.

[28] John, P.; Purnell, J. H. *J. Chem. Soc., Faraday Trans. 1* **1973**, *69*, 1455.

[29] Vanderwielen, A. J.; Ring, M. A.; O'Neal, H. E. *J. Am. Chem. Soc.* **1975**, *97*, 993.

[30] Ball, D. F.; Carter, T.; McKean, D. C.; Woodward, L. A. *Spectrochim. Acta* **1964**, *20*, 1721.

Table VII. Reaction Scheme for the Thermolysis of $MeSiH_3$

reaction step	log A^a	E_a, kcal mol^{-1}
Molecular Process		
$MeSiH_3 \rightarrow MeSiH{:} + H_2$ (1a)	14.87 ± 0.12^b	63.15 ± 0.35^b
$MeSiH{:} + MeSiH_3 \rightleftarrows (MeSiH_2)_2$ (2; −2)	10; 14^c	~ 0; 50^c
Radical Process		
Initiation		
$MeSiH_3 \xrightarrow{wall} MeSiH_2^{\bullet} + H^{\bullet}$ (1b)	$\sim 12.7^b$	57.9^b
(a) No Ethylene		
Propagation		
$H^{\bullet} + MeSiH_3 \rightarrow H_2 + MeSiH_2^{\bullet}$ (3)	10.2^c	2.1^c
$MeSiH_2^{\bullet} + MeSiH_3 \rightarrow (MeSiH_2)_2 + H^{\bullet}$ (4)	$\sim 9^c$	$\sim 17^c$
Termination		
$2MeSiH_2^{\bullet} \rightarrow (MeSiH_2)_2$ (5)	$\sim 9.5^c$	$\sim 0^c$
$MeSiH_2^{\bullet} \xrightarrow{wall}$ polymer (6)		
$CH_3SiH_2^{\bullet} \xrightarrow{X(wall)} Me_2SiH_2$ (7)		
(b) Ethylene Added		
$H^{\bullet} + C_2H_4 \rightarrow C_2H_5^{\bullet}$ (8)	10.0^c	2.1^c
$MeSiH_2^{\bullet} + C_2H_4 \rightarrow MeSiH_2CH_2CH_2^{\bullet}$ (9)	$\sim 8.0^c$	$\sim 1.4^c$
$MeSiH{:} + C_2H_4 \rightarrow$ SiHMe (10)		
$C_2H_5^{\bullet} + MeSiH_3 \rightarrow C_2H_6 + MeSiH_2^{\bullet}$ (11)		
$MeSiH_2CH_2CH_2^{\bullet} + MeSiH_3 \rightarrow MeSiH_2CH_2CH_3 + CH_3SiH_2^{\bullet}$ (12)		

[a] A factors for unimolecular and bimolecular reactions are in units of s^{-1} and M^{-1} s^{-1}, respectively. [b] Measured in this work. [c] Estimated, or reported in the literature. See text.

This agreement shows that the cyclic structure is a reasonable assumption.

Free Radical Process. The H_2 fractions resulting from purely radical processes can be obtained by subtracting the molecular H_2 yields calculated from the Arrhenius expression for step 1a from the total H_2 yields, listed in Table II. The H_2 reaction orders for the radical reactions, Table IV, vary between 1.6 and 2.0, in the expected range for a radical chain. From the data in Table III the reaction orders for DMDS(rad) and DMS are 1.40 ± 0.17 and 1.59 ± 0.09, respectively, at 415 °C.

In the reaction scheme shown in Table VII the two major chain-propagating steps

$$H^{\bullet} + CH_3SiH_3 \rightarrow H_2 + CH_3SiH_2^{\bullet} \tag{3}$$

$$CH_3SiH_2^{\bullet} + CH_3SiH_3 \rightarrow \text{DMDS} + H^{\bullet} \tag{4}$$

most easily satisfy the requirements for the generation of H_2 and DMDS in a radical chain mechanism. Displacement reaction 4 is proposed by analogy with the (reverse) reaction[18]

$$H^{\bullet} + Si_2H_6 \rightarrow SiH_3^{\bullet} + SiH_4$$

Owing to the high estimated value of E_4, reaction 4 can only proceed at elevated temperatures: thus, in the $Hg(^3P_1) + CH_3SiH_3$ system, which generates $H^{\bullet}$ atoms and $CH_3SiH_2^{\bullet}$ radicals,[10] $\phi(H_2) = 0.81$ at room temperature, clearly precluding the occurrence of a chain mechanism.

If a long chain is operative, the rates of propagating steps 3 and 4 are of comparable magnitude. Hence at 400 °C

$$\frac{[CH_3SiH_2^{\bullet}]}{[H^{\bullet}]} \sim \frac{k_3}{k_4} \sim \frac{3.31 \times 10^9}{3.02 \times 10^3} \sim 1.1 \times 10^6$$

and the chain will be terminated almost exclusively by $CH_3SiH_2^{\bullet}$ radicals.

The reaction order for the products of a long-chain reaction will depend mainly on the type of termination of the chain. The usual steady-state approximations predict that the reaction orders for H_2(rad) and DMDS(rad) will be 1.5 if the chain is terminated quadratically by

$$2CH_3SiH_2 \rightarrow \text{DMDS} \tag{5a}$$

$$\rightarrow CH_2{=}SiH_2 + CH_3SiH_3 \tag{5b}$$

or 2 if the chain termination is linear:

$$CH_3SiH_2^{\bullet} \xrightarrow{wall} \text{polymer} \tag{6}$$

$$CH_3SiH_2^{\bullet} \xrightarrow{X(wall)} \text{DMS} \tag{7}$$

The experimental reaction orders for H_2(rad), Table IV, are somewhat scattered, yet are closer to 2 than to 1.5.

Note that only recombination step 5a is listed in Table VII since the occurrence of disproportionation ($k_d/k_c \sim 0.1$ at 25 °C[31]) would not alter the overall kinetics.

As shown by the C_2H_4 scavenging experiments, DMS is formed from a radical precursor, the most likely being $CH_3SiH_2^{\bullet}$, and the results in Table I (case C) suggest that DMS is formed at least partly in a heterogeneous process. Therefore, reaction 7 may best explain experimental observations, with the chemisorbed species X being either the substrate or some undefined species $C_xSi_yH_z$ such as those produced by thermolysis of the $CH_3SiH_2^{\bullet}$ radical (Scheme I). The other linear chain breaking step, (6), is an additional reaction generating polymer.

For conversions in excess of 1%, the rate of formation of DMS increases while that of DMDS decreases (Table I, case A). Under these conditions, it appears that DMDS undergoes thermolysis, giving DMS

$$CH_3SiH_2{-}SiH_2CH_3 \xrightarrow{\Delta} (CH_3)_2SiH_2$$

in a process that probably features a radical component and may be occurring on the wall. The elucidation of this source of DMS will require a detailed examination of the thermolysis of DMDS and will have to wait until this information becomes available.

Owing to the possibility of quadratic (step 5) and linear (steps 6 and 7) chain breaking steps, the overall kinetics of decomposition are exceedingly complex. Some useful information can be gained, however, by considering the two possibilities separately. Thus, if the chain is terminated quadratically, the rate expressions are

$$R_{H_2}^{\text{tot}} = (k_{1a} + k_{1b})_{\text{quad}}[\text{MMS}] + \left\{k_4\left(\frac{k_{1b}}{k_5}\right)^{1/2}\right\}_{\text{quad}}[\text{MMS}]^{3/2} \tag{21}$$

$$R_{\text{DMDS}}^{\text{tot}} = (k_{1a} + k_{1b})_{\text{quad}}[\text{MMS}] + \left\{k_4\left(\frac{k_{1b}}{k_5}\right)^{1/2}\right\}_{\text{quad}}[\text{MMS}]^{3/2} - R_{\text{polymer}} \tag{22}$$

$$R_{\text{DMS}} = \left\{k_7\left(\frac{k_{1b}}{k_5}\right)^{1/2}\right\}_{\text{quad}}[\text{MMS}]^{3/2} \tag{23}$$

Similarly, for linear termination

---

[31] Gammie, L.; Safarik, I.; Strausz, O. P.; Roberge, R.; Sandorfy, C. *J. Am. Chem. Soc.* **1980**, *102*, 378.

$$R_{H_2}{}^{tot} = (k_{1a} + k_{1b})_{lin}[MMS] + \left\{k_4 \frac{2k_{1b}}{k_6 + k_7}\right\}_{lin} [MMS]^2 \quad (24)$$

$$R_{DMDS}{}^{tot} = k_{1a_{lin}}[MMS] + \left\{k_4 \frac{2k_{1b}}{k_6 + k_7}\right\}_{lin} [MMS]^2 - R_{polymer} \quad (25)$$

$$R_{DMS} = \left\{k_7 \frac{2k_{1b}}{k_6 + k_7}\right\}_{lin} [MMS]^2 \quad (26)$$

The kinetic expressions for R_{H_2}, (21) and (24), are mathematically the most simple and since the experimental data on H_2 are extensive and accurate, a more detailed analysis of the kinetics of H_2 formation offers the possibility of differentiating between the two chain termination mechanisms.

Rearranging (21) and (24) gives

$$\frac{R_{H_2}{}^{tot}}{[MMS]} = (k_{1a} + k_{1b})_{quad} + \left\{k_4\left(\frac{k_{1b}}{k_5}\right)^{1/2}\right\}_{quad} [MMS]^{1/2} \quad (27)$$

and

$$\frac{R_{H_2}{}^{tot}}{[MMS]} = (k_{1a} + k_{1b})_{lin} + \left\{k_4 \frac{2k_{1b}}{k_6 + k_7}\right\}_{lin} [MMS] \quad (28)$$

Equations 27 and 28 predict a linear relationship between $R_{H_2}{}^{tot}/[MMS]$ and $[MMS]^{1/2}$ and [MMS], respectively, and identical intercepts yielding $k_{1a} + k_{1b}$.

Unfortunately, the resulting kinetic plots (using the data in Tables II and III) are not sensitive enough to differentiate between the two different kinetic behaviors and they both yield the predicted linear relationships. Two representative examples of these kinetic plots are illustrated in Figure 3. Therefore, they do not offer a straightforward choice between the two possible mechanisms.

The first-order rate coefficients corresponding to the intercepts of eq 27 and 28 were determined by least mean squares analyses of these kinetic plots, and the results are listed in Table VIII along with the values of k_{1a} obtained from the Arrhenius parameters that were already determined in separate sets of experiments. Therefore k_{1b} can be obtained by simple subtraction of k_{1a} from $(k_{1a} + k_{1b})$. Values of k_{1b} are listed in Table VIII for both the quadratic and linear cases. It is seen that the k_{1b} values derived for the quadratic case are widely scattered and about half of them are negative, indicating that the experimental results are not consistent with the assumption of quadratic termination of the chain. On the other hand, the k_{1b} values derived for the linear case show a monotonous decrease with decreasing temperature, and the plot of log k_{1b} vs. $1/T$, Figure 4, has a very good linear correlation with the following Arrhenius parameters:

$$\log k_{1b} = (12.71 \pm 0.51) - (57860 \pm 1560)/2.3RT$$

The low values of the activation energy ($D(CH_3SiH_2{-}H) \sim 89.6$ kcal mol^{-1} [12]) and preexponential factor are consistent with a surface-catalyzed reaction. If the values of k_{1b}, calculated from the above rate expression, Table IX, are compared with the values of k_{1b} listed in Table V, which were obtained from the $R_{H_2} - R_{DMDS}$ difference in the inhibited reaction (Figure 1), assuming that the "excess" hydrogen comes from radical steps 1b and 3, it is seen that they generally agree within a factor of 2. Considering the fact that the latter were derived from the difference between two numbers of comparable magnitude, thus ensuring large errors, we consider the agreement to be entirely satisfactory and these results further support our[4] and RPO's[2] earlier proposal of dual molecular and radical initiating steps in the thermolysis of MMS.

More insight into the nature of the chain-breaking mechanism can be achieved from the kinetic analysis of the rate constant ratio $[k_4(2k_{1b}/(k_6 + k_7)]_{lin}$, derived from least mean squares analysis of the slopes of eq 28. From these values, listed in Table IX, along with the calculated values of k_{1b} and k_4, the corresponding $(k_6 + k_7)$ values were derived. The plot of log $(k_6 + k_7)$ vs. $1/T$ gave a good straight line, Figure 4, from which log $A = 11.7$ and $E_a = 32.3$ kcal mol^{-1}. For an Arrhenius type plot involving two rate constants, there are two conditions which, if satisfied, would lead to a linear plot: (a) $A_6 \neq A_7$ and $E_6 \simeq E_7$: $\log (k_6 + k_7) = \log (A_6 + A_7) - E_{av}/2.3RT$; (b) $A_6 \ll A_7$: $\log (k_6 + k_7) \simeq \log A_7 - E_7/2.3RT$. At present we cannot distinguish between these two possibilities but in view of the fact that, for $(CH_3)_2Si$: radicals, $E_6 = 0$ and log $A_6 \sim 5$,[22] condition b appears to be more reasonable. In any case the low value of $E_a \sim 32$ kcal mol^{-1} is in agreement with our earlier conclusion that DMS is a surface-catalyzed product.

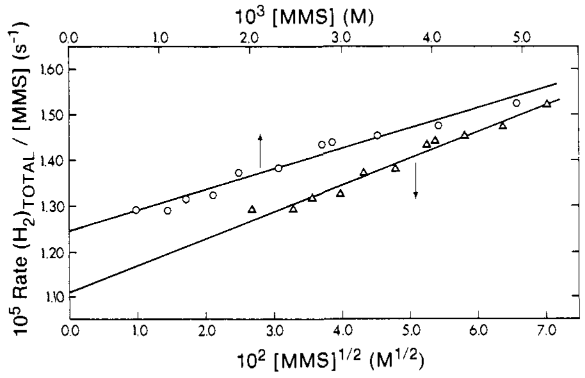

Figure 3. $R_{H_2}{}^{tot}/[MMS]$ vs. $[MMS]^{1/2}$ (○) and [MMS] (△) at 421 °C.

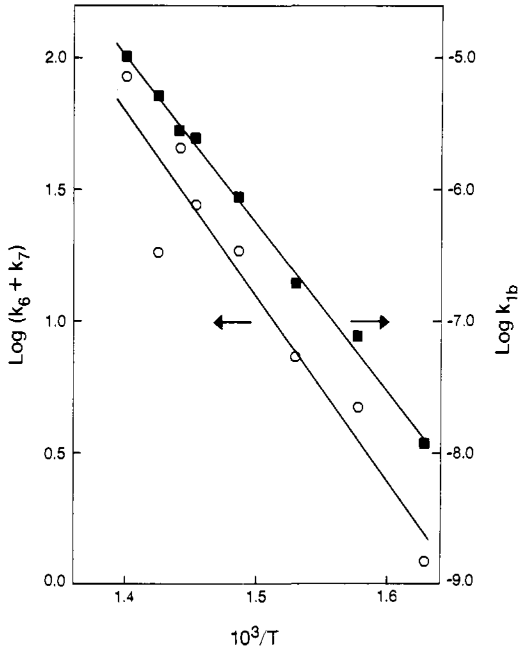

Figure 4. log k_{1b} (■) and log $(k_6 + k_7)$ (○) vs. $1/T$ for linear termination kinetics.

The length of the radical chain λ can be estimated from

$$\lambda = R(\text{propagation})/R(\text{termination})$$

where R(propagation) can be approximated by $R_{H_2}{}^{rad}$ provided the chain is sufficiently long.

For linear termination of the chain

$$R(\text{termination}) = (k_6 + k_7)[CH_3\dot{S}iH_2]$$

and, from steady-state treatment of the overall mechanism

$$[CH_3\dot{S}iH_2] = 2k_{1b}[MMS]/(k_6 + k_7)$$

After substitution

$$R(\text{termination}) = 2k_{1b}[MMS] = 4.0 \times 10^{-8}\ M^{-1}\ s^{-1}$$

Table VIII. Rate Constants k_{1b} as a Function of Temperature for Linear and Quadratic Chain Termination

		$k_{1a} + k_{1b}$, s^{-1}		k_{1b}, s^{-1}	
T, °C	k_{1a},[a] s^{-1}	quadratic[b]	linear[c]	quadratic	linear
441	3.47×10^{-5}	$(4.26 \pm 0.17) \times 10^{-5}$	$(4.47 \pm 0.08) \times 10^{-5}$	7.90×10^{-6}	1.00×10^{-5}
429	1.62×10^{-5}	$(1.61 \pm 0.18) \times 10^{-5}$	$(2.14 \pm 0.09) \times 10^{-5}$	-1.00×10^{-7}	5.20×10^{-6}
421	9.77×10^{-6}	$(1.11 \pm 0.02) \times 10^{-5}$	$(1.25 \pm 0.01) \times 10^{-5}$	1.33×10^{-6}	2.73×10^{-6}
415	6.46×10^{-6}	$(6.24 \pm 1.02) \times 10^{-6}$	$(8.84 \pm 0.63) \times 10^{-6}$	-2.20×10^{-7}	2.38×10^{-6}
400	2.34×10^{-6}	$(2.61 \pm 0.19) \times 10^{-6}$	$(3.24 \pm 0.11) \times 10^{-6}$	2.70×10^{-7}	9.00×10^{-7}
381	5.89×10^{-7}	$(4.98 \pm 0.96) \times 10^{-7}$	$(7.83 \pm 0.38) \times 10^{-7}$	-9.10×10^{-8}	1.94×10^{-7}
361	1.26×10^{-7}	$(1.30 \pm 0.34) \times 10^{-7}$	$(2.03 \pm 0.21) \times 10^{-7}$	4.00×10^{-9}	7.70×10^{-8}
341	2.51×10^{-8}	$((-2.78 \pm 1.00) \times 10^{-8})$[d]	$(3.68 \pm 0.12) \times 10^{-8}$		1.17×10^{-8}

[a] Calculated from log $k_{1a} = 14.87 - 63150/2.3RT$. [b] Intercept of eq 27. [c] Intercept of eq 28. [d] Only three experiments.

Table IX. Rate Constants as a Function of Temperature for Linear Termination of the Chain

T, °C	$k_4[2k_{1b}/(k_6 + k_7)]_{\text{lin}}$,[a] M^{-1} s^{-1}	k_{1b},[b] s^{-1}	k_4,[c] M^{-1} s^{-1}	$(k_6 + k_7)$, s^{-1}
441	$(1.46 \pm 0.37) \times 10^{-3}$	1.00×10^{-5}	6.17×10^{3}	84.52
429	$(2.74 \pm 0.35) \times 10^{-3}$	5.01×10^{-6}	5.01×10^{3}	18.32
421	$(5.95 \pm 0.40) \times 10^{-4}$	3.09×10^{-6}	4.36×10^{3}	45.28
415	$(6.07 \pm 1.14) \times 10^{-4}$	2.14×10^{-6}	3.89×10^{3}	27.43
400	$(2.64 \pm 0.36) \times 10^{-4}$	8.32×10^{-7}	2.95×10^{3}	18.59
381	$(1.34 \pm 0.11) \times 10^{-4}$	2.40×10^{-7}	2.04×10^{3}	7.31
361	$(3.34 \pm 1.11) \times 10^{-5}$	5.89×10^{-8}	1.35×10^{3}	4.76
341	$(1.88 \pm 0.03) \times 10^{-5}$	1.32×10^{-8}	8.71×10^{2}	1.22

[a] Slope of eq 28. [b] Calculated from log $k_{1b} = 12.71 - 57860/2.3RT$. [c] Calculated from log $k_4 = 9.0 - 17000/2.3RT$.

at 415 °C and [MMS] = 9.44×10^{-3} M (405 Torr). From the decrease in $R_{H_2}{}^{\text{tot}}$ in the presence of C_2H_4, Figure 1, the rate of propagation, $R_{H_2}{}^{\text{rad}}$, = 1.8×10^{-7} M^{-1} s^{-1} under the same conditions and thus

$$\lambda = \frac{1.8 \times 10^{-7}}{2.8 \times 10^{-8}} = 4.5$$

This is in agreement with the value for λ obtainable directly from Figure 1

$$\lambda = \frac{R_{H_2}{}^{\text{tot}} - R_{H_2}{}^{\text{inhib}}}{R_{H_2}{}^{\text{inhib}} - R_{\text{DMDS}}{}^{\text{inhib}}} \approx 5.5$$

where the excess H_2 is at least partly due to the H_2 produced in the thermolysis of the polysilane polymer (Scheme I). This estimate of the chain length is several orders of magnitude lower than the one we estimated earlier[4] and confirms SOR's[6] suggestion that the chain length is relatively short.

To summarize, our results show conclusively that under conditions of moderate pressure, low conversion, and in the temperature range 340–440 °C, MMS decomposes primarily by geminal molecular elimination of H_2 from the silicon moiety to generate methylsilylene, which then inserts into the Si–H bond of MMS to yield the other major product, DMDS. These reactions could be clearly delineated from experiments carried out in the presence of added C_2H_4, which suppresses DMDS formation from $CH_3SiH_2^{\bullet}$ precursors. The rate parameters obtained for the formation of H_2 and DMDS were similar as long as the conversions were kept low. In addition to molecular elimination of H_2 there is also a slow, surface-catalyzed decomposition yielding $H^{\bullet} + CH_3SiH_2^{\bullet}$ and a short-chain reaction involving these two radicals is set up, yielding additional amounts of H_2 and DMDS and also small amounts of DMS produced on the reactor surface. From kinetic analysis of the H_2 yields we were able to derive rate parameters for the radical primary step and to establish that the chain is terminated by two linear steps, both surface catalyzed, one leading to the formation of DMS. It was also clearly established that the decomposition of the DMDS product affords DMS which, in high-conversion experiments, can obscure the primary products and primary thermolysis steps. This high sensitivity of the reaction to surface effects and extent of conversion appears to offer the most plausible explanation for the discrepancy in the experimental results and the interpretation of the reaction mechanism in earlier reports.

Acknowledgment. We thank the Natural Sciences and Engineering Research Council of Canada for continuing financial support.

Note Added in Proof: Professor M. A. Ring has kindly read the manuscript and agrees with us that the discrepancies between our work and his[6] are due to the different extents of conversion.